THE UNIVERSITY OF MICHIGAN

College of Engineering

Department of Nuclear Engineering

Laboratory for Fluid Flow and Heat Transport Phenomena

Report No. 07738-5-T

NUMERICAL AND PHOTOGRAPHIC STUDIES

OF ASYMMETRIC BUBBLE COLLAPSE

T. M. Mitchell
C. L. Kling
R. Cheesewright
F. G. Hammitt

July 1967

ABSTRACT

Recent investigations of the fundamental aspect of cavitation damage have indicated the importance of asymmetric bubble collapse. This investigation is an effort to theoretically and experimentally justify the role of asymmetric bubble collapse in cavitation damage. The theoretical investigation employs a combined Eulerian and Lagrangian computer code capable of following the collapse of a bubble much further than previous perturbation techniques. The experimental investigation is concerned with the development of a specialized spark camera with a maximum framing rate of 10^6 frames per second and a spatial resolution higher than any other camera presently available at this laboratory.

TABLE OF CONTENTS

LIST OF FIGURES

Page

THE ASYMMETRIC COLLAPSE OF CAVITATION BUBBLES

Introduction:

Over the last few years, interest in the fundamental aspect of

cavitation which is concerned with the collapse of a single isolated

bubble has moved away from the classic concept of symmetrical collapse

exemplified by the work of Rayleigh (1), Hickling and Plesset (2), Ivany

and Hammitt (3), etc. Following an initial suggestion by Kornfeld and

Suvorov (4) and important work by Rattray (5), Naude and Ellis (6),

and Shutler and Mesler (7), attention has been increasingly directed

towards the consideration of asymmetric collapse phenomena.

This interest in the asymmetric collapse mode is justified by

general considerations of the collapse phenomena (e.g., Benjamin and

Ellis (8)), as well as the experimental evidence of Ivany, Hammitt, and

Mitchell (9), Shutler and Mesler (7), etc., and analytical considerations

of the early stages of the collapse phenomena by Rattray (5), Naude and

Ellis (6), and Yeh (10), which have all shown a tendency for the cavi-

tation bubble to become asymmetric during the collapse. These latter

theoretical considerations have all made use of perturbation techniques

based on the classical symmetric solution, and have therefore been limited

to relatively small departures from spherical symmetry.

One aspect of the present investigation is aimed at extending the

theoretical considerations of the asymmetric collapse phenomena to much

later stages of collapse than is possible with perturbation techniques. With this object in view, a study has been made of some of the powerful techniques which have been developed over the last few years for solving complex fluid mechanics problems using a high speed digital computer. The first part of this report describes the results of this study which led to the choice of the MAC (Marker and Cell) method as being the most suitable for the problem in hand. This method was first applied to the classic problem of symmetric collapse in order to gain a feeling for the problems involved in its application to problems of bubble collapse. The results of this preliminary investigation and their implications with regard to the study of the asymmetric collapse, which is presently under way, are reported.

Another aspect of this present investigation which is concerned with obtaining more accurate and more detailed experimental data on the asymmetric collapse phenomena is contained in the second part of this report. This part is mainly concerned with the development of a special camera having sufficient spatial and temporal resolution to record the details of the bubble collapse on film.

Theoretical Considerations:

In selecting a suitable technique for the calculation of the asymmetric mode of bubble collapse, consideration was given to the long term objectives. These long term aims include the desirability of being able to consider the effect of such factors as bubble gas content, fluid viscosity,

arbitrary pressure gradients, and the presence of a solid wall, whereas the short term objective is merely to study the asymmetric collapse of a vapour bubble in an infinite volume of perfect fluid, subject to a step change in fluid pressure.

The selection of the most suitable technique is at first a matter of elimination. The non-linearity of the partial differential equations together with the free surface boundary condition precludes a direct analytic solution. Numerical solution of the difference equations with an Eulerian (stationary) grid cannot handle the free surface condition. A purely Lagrangian numerical solution, on the other hand, will not adequately describe a fluid flow in the presence of large distortions such as may be anticipated in the asymmetric collapse problem.

A combination of the Eulerian and Lagrangian approaches could offer some of the advantages of both methods while overcoming some of the disadvantages. One example of the combined approach is the Particle-in-Cell (PIC) method (11), developed by Harlow at Los Alamos. This method, which was initially developed for use in compressible flow problems, was discarded because it requires that no part of the flow be far subsonic, a condition which is untrue for most of the bubble collapse problem.

The eventual choice for the appropriate method came to be the Marker-and-Cell (MAC) method developed by Harlow and Welch at Los Alamos (12). This method appears to have worked very well for solution of a variety of problems involving incompressible liquids with free surfaces. It requires a high-speed computer with extensive storage capacity.

With the eventual solution of the asymmetric problem in mind, we have first applied the MAC method to the problem of the spherical collapse of a cavitation bubble (Rayleigh's problem), because an analytic solution already exists for this problem and we can thus determine the characteristics of this technique as applied to bubble collapse problems and the effect of such parameters as grid sizes and time interval.

The MAC method starts with an Eulerian grid as shown in Figure 1 (a). Field variables such as pressure and velocity are directly associated with the cells of the grid. In addition to the grid, a series of marker particles are assigned to the liquid; these particles do not participate in the dynamics of the problem and are essentially "massless", but they are necessary to take care of the free surface movement.

Although the Los Alamos work suggests that marker particles be located throughout the liquid initially, experience with the symmetric collapse problem has shown that a considerable saving in computer time and storage can be obtained by starting with particles located only along the free surface. This arrangement is possible because of the condition (see Lamb (13)) that fluid particles initially on the free boundary always remain on the free boundary.

In the spherically symmetric case, the above considerations lead to the use of one single particle (marked A in Figure 1 (a)) to define the free boundary. In the asymmetric case it is intended to start with particles located along the free boundary as in Figure 1 (b).

θ

r
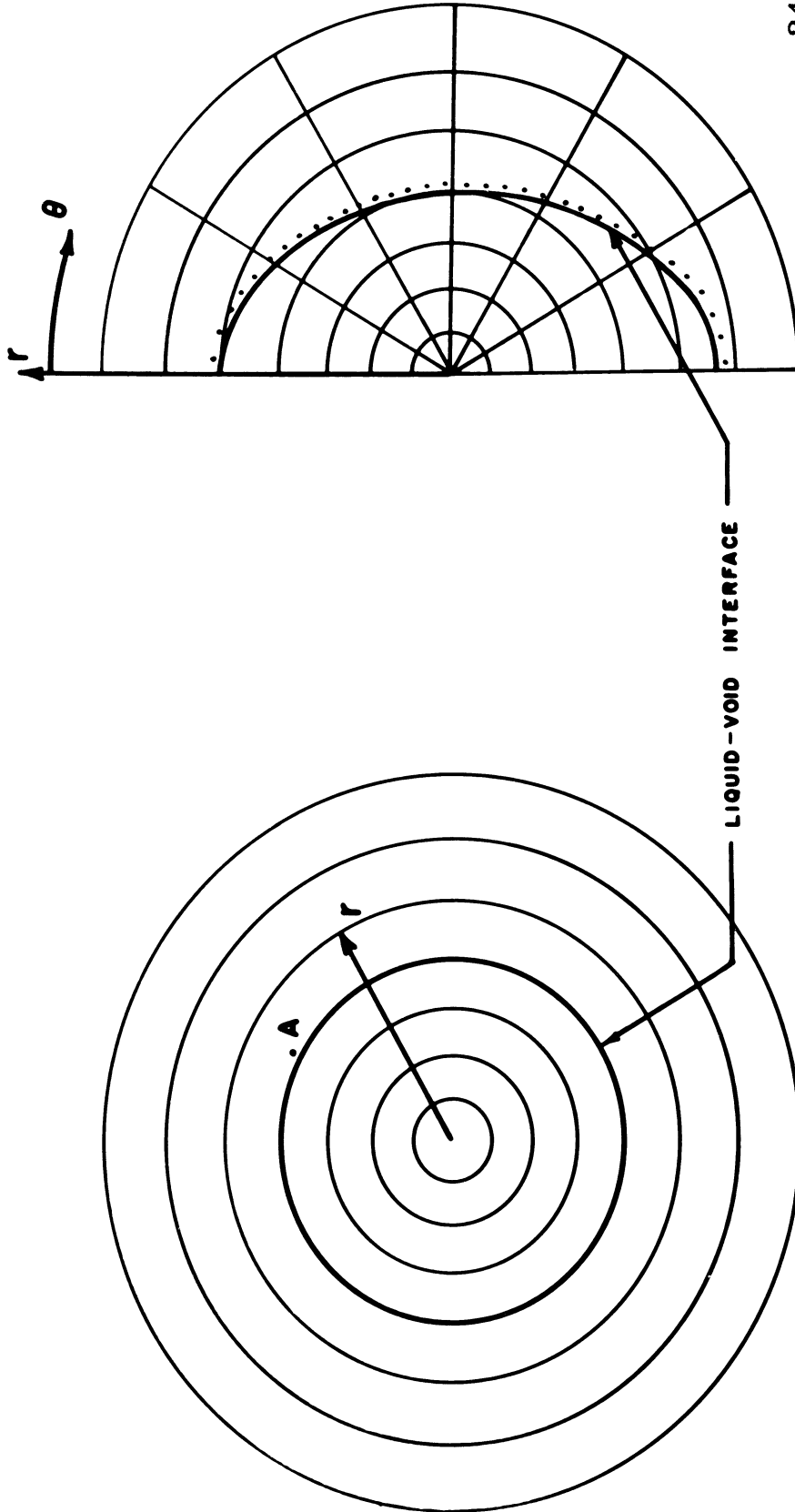
2488

Fig. 1(b)--Grid and Initial
Marker Particle Locations for MAC
Solution of the Axially Symmetric
(Two-Dimensional) Problem.

LIQUID-VOID INTERFACE

r

.A

Fig. 1(a)--Grid and Initial
Marker Particle Location for MAC
Solution of the Spherically Sym-
metric (One-Dimensional) Problem.

To explain the technique in more detail, it is convenient to take as the starting point of the problem, the hydrodynamic equations for continuity and conservation of momentum, in one-dimensional spherical coordinates:

$$\frac{\partial}{\partial \hbar} \left(\hbar^2 u \right) = 0 \tag{1}$$

$$\frac{\partial u}{\partial t} + \left(\vec{u} \cdot \vec{\nabla} \right) \vec{u} = -\frac{\partial P}{\partial \hbar} \tag{2}$$

where u = the radial velocity in the liquid, $P = \frac{p}{\rho}$, p is the liquid pressure, and ρ is the liquid density (constant for the incompressible problem).

The boundary conditions for the problem are:

$$P = P_\infty \quad \text{AS} \quad \hbar \rightarrow \infty \; ; \tag{3}$$

$$P = 0 \quad \text{FOR} \quad \hbar \leq R(t), \tag{4}$$

where R is the radius of the bubble wall;

$$R(0) = R_0 \tag{5}$$

$$\frac{dR}{dt}(0) = 0 \tag{6}$$

Equation (2) can be rewritten as

$$\frac{\partial u}{\partial t} + \frac{1}{2} \frac{\partial (u^2)}{\partial \hbar} = -\frac{\partial P}{\partial \hbar} \tag{7}$$

Harlow and Welch point out that this transformation is essential for rigorous momentum conversation after the equations are written in difference form.

The cells of the grid system are then labeled with an index i; further, the P-quantity $(=p/\rho)$ is defined at the center of each cell as P_i and the velocities are defined on the cell-boundaries as $u_{i-1/2}$ and $u_{i+1/2}$. The definition of these quantities at any other locations increases the complexity of the calculation and brings in values from "far-distant" points, thus contributing to increased inaccuracy.

It is then possible to write equation (1) in difference form as:

$$D_i = 0 \qquad (8)$$

$$\text{IF} \quad D_i \triangleq \frac{1}{\Delta R} \left([R^2 u]_{i+1/2} - [R^2 u]_{i-1/2} \right)$$

$$\text{WHERE} \quad \Delta R = R_{i+1/2} - R_{i-1/2}$$

Equation (7) similarly becomes

$$\frac{1}{\delta t} \left(u^{n+1}_{i+1/2} - u_{i+1/2} \right) = \frac{1}{2} \left(\frac{u_i^2 - u_{i+1}^2}{\Delta R} \right) + \left(\frac{P_i - P_{i+1}}{\Delta R} \right) \qquad (9)$$

The superscript n+1 indicates that the quantity is evaluated at $t = (n+1)\,\delta t$ while the absence of a superscript indicates that the evaluation is at $t = n\,\delta t$. The quantity $\bar{u}_i$ is defined as $1/2(u_{i+1/2} + u_{i-1/2})$. If, in addition, equation (8) is rewritten for D_i^{n+1} and (9) is rewritten for $u_{i-1/2}^{n+1}$, and the resulting four equations are combined, one obtains

$$\frac{1}{\delta t}\left(D_i^{n+1}-D_i\right) = \frac{1}{(\Delta n)^2}\left[n_{i+\frac{1}{2}}^2\left(P_i-P_{i+1}\right)-n_{i-\frac{1}{2}}^2\left(P_{i-1}-P_i\right)\right]$$

$$+ \frac{1}{(\Delta n)^2}\left[\frac{n_{i+\frac{1}{2}}^2}{2}\left(u_i^2-u_{i+1}^2\right)-\frac{n_{i-\frac{1}{2}}^2}{2}\left(u_{i-1}^2-u_i^2\right)\right] \tag{10}$$

Equations (9) and (10) provide the basis of the computational method.

Knowing the pressure distribution at any time t, equation (9) is solved

to give the velocity distribution at t+δ t; equation (10) can then be

solved, assumed D_i^{n+1}= 0,to give the pressure distribution at time

t+δ t.

Two questions arise in connection with this scheme of computation.

The first is concerned with the initial conditions to be imposed at

t = 0.   Strictly this should be P = P_∞ for r $>$ R_0 at t = 0.   Because

of the computational scheme, however, the pressure discontinuity

initially at the bubble wall would require a finite time to propagate

out through the liquid and thus would violate the assumption of an

incompressible fluid.   In the symmetric case this difficulty has been

overcome by the use initially of the pressure distribution as given by

the Rayleigh solution.   In the asymmetric case it is felt that it will

be necessary to begin with either the Rayleigh solution or perhaps the

results of a perturbation solution (Rattray, Yeh, etc.) for small degrees

of asymmetry.

The second question concerns the boundary condition at the outer

extremity of the grid system.   The true boundary condition in the Rayleigh

problem is that P is specified at infinity. Since we are forced to use a grid system of finite extent, it is not possible to employ this condition. To overcome this difficulty, the pressure predicted by the Rayleigh solution has been used as the boundary condition at the outer edge of the grid system. It is proposed to use the same procedure in the asymmetric collapse problem.

After solving equations (9) and (10) for the velocity and pressure distributions for time $t + \delta t$, the marker particle is moved. The movement is accomplished by looking at the present location of the particle, interpolating between the velocities at the boundaries of the cell in which the particle is located to find the particle velocity, and then moving the particle a distance equal to this velocity times δt. The procedure then is to scan the grid to see if the particle has moved into another cell and, if so, to incorporate the new cell into the succeeding Eulerian calculations. After printing any necessary output-data, the cycle of calculations is repeated.

The primary goal of the study of the spherical bubble problem by the MAC method has been the investigation of the effects of different grid sizes and time intervals. 25 and 40 cell grids were used for two different sets of calculations. Use of the 40 cell grid reduced the error in the initial stages of the calculation by about 1/3 from that with the 25 cell grid, at a cost of a 20% increase in computing time.

At later stages in the collapse, however, the error improvement dis-
appeared, although this was masked by the constant time step error
explained below.

Two problems were apparent when constant time steps of 5 and
10 us were utilized. In the late stages of collapse, the bubble wall
velocity diverged rapidly from the expected Rayleigh value. This
difficulty arose apparently because of stability considerations violated
when the particle moved across a large part of a cell in one time
interval. This difficulty was overcome by varying the time interval
so as to impose a maximum on the particle movement in one time cycle
of 10% of a single cell width.

The other difficulty concerned the error in the early stages of the
collapse. This error is dependent on both grid size and time increment,
but a method of reducing this error without involving a large increase
in computing time, has not yet been achieved. The error does, however,
appear to die out with time and so possibly may be ignored in the
asymmetric case.

A check on the accuracy of the computed results can be made by
comparing the results with corresponding values calculated from Rayleigh's
analytical solution. Figure 2 shows a plot of the bubble wall radius vs.
time. The solid line indicates the Rayleigh solution; the data points
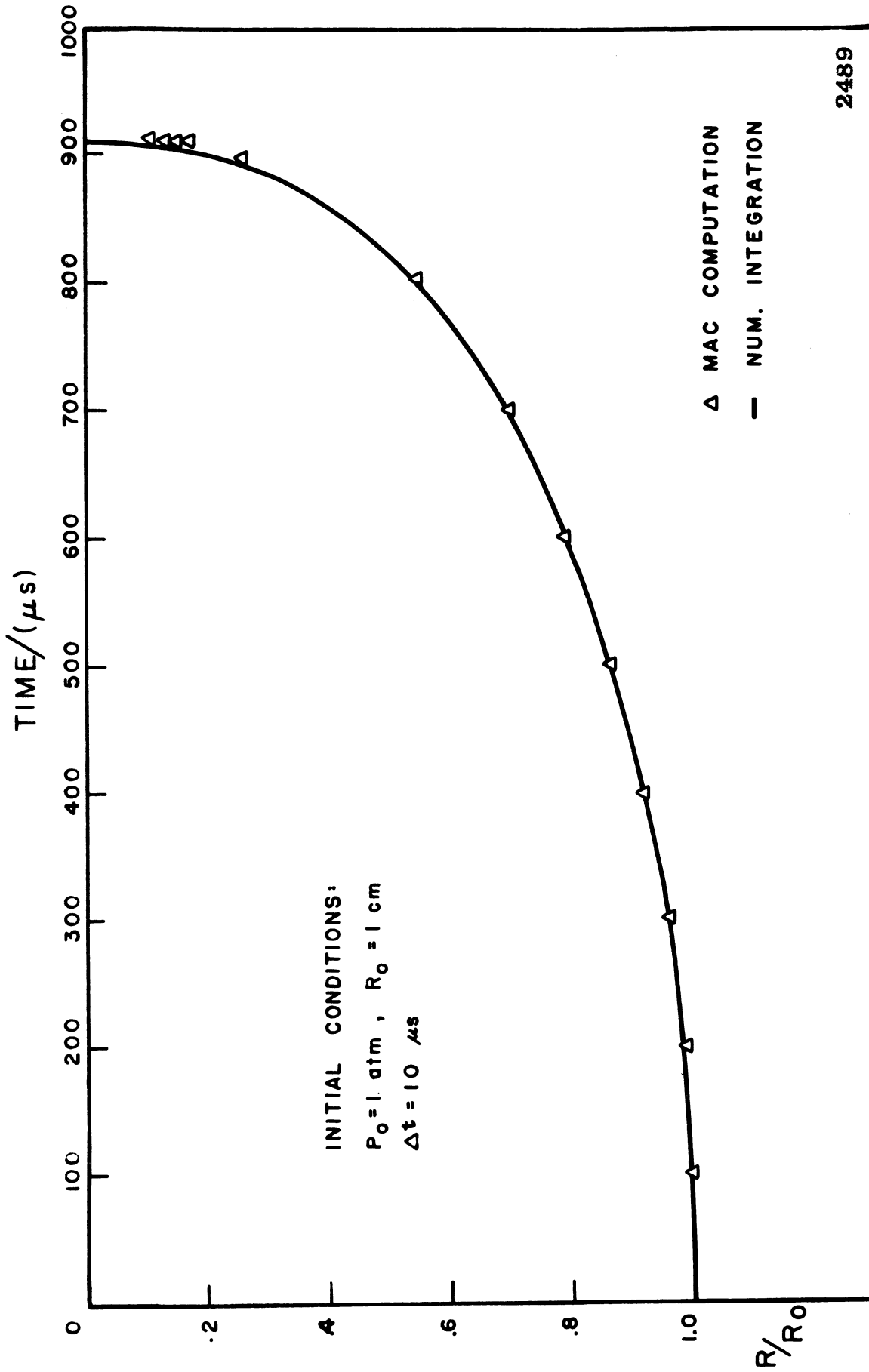are those obtained from the Marker-and-Cell program. The MAC method

Fig. 2.--Comparison of Radius as a Function
of Time by Two Methods: MAC and Simpson's Rule
Numerical Integration.

data virtually coincides with the Rayleigh results except for a slight divergence at the very end of collapse. Figure 3 shows another comparison of the two methods expressed in terms of the percentage error as a function of time (the percentage error is defined here as the difference between the Rayleigh velocity for the present bubble radius and the MAC velocity divided by the Rayleigh velocity). The curves of Figure 3 show the improvement arising from using a variable time step rather than one of constant value and also the problem of the initial error.

It is hoped that the following conclusions drawn from the study of the spherically symmetric case can be applied to the axially-symmetric two-dimensional case:

1. Marker particles need only be located initially along the liquid-cavity interface.

2. A variable time step is necessary for accuracy.

3. For greatest accuracy, some initally correct pressure distribution should be imposed upon the liquid.

4. Approximately 25 cells radially are sufficient to give an accuracy of the order of 5%. It is hoped that this can be improved further by correcting the initial error problem.

5. The pressure in the one cell necessarily external to the grid system must be controlled by an appropriate expression, possibly the correct Rayleigh pressure as was used in the spherically symmetric case.
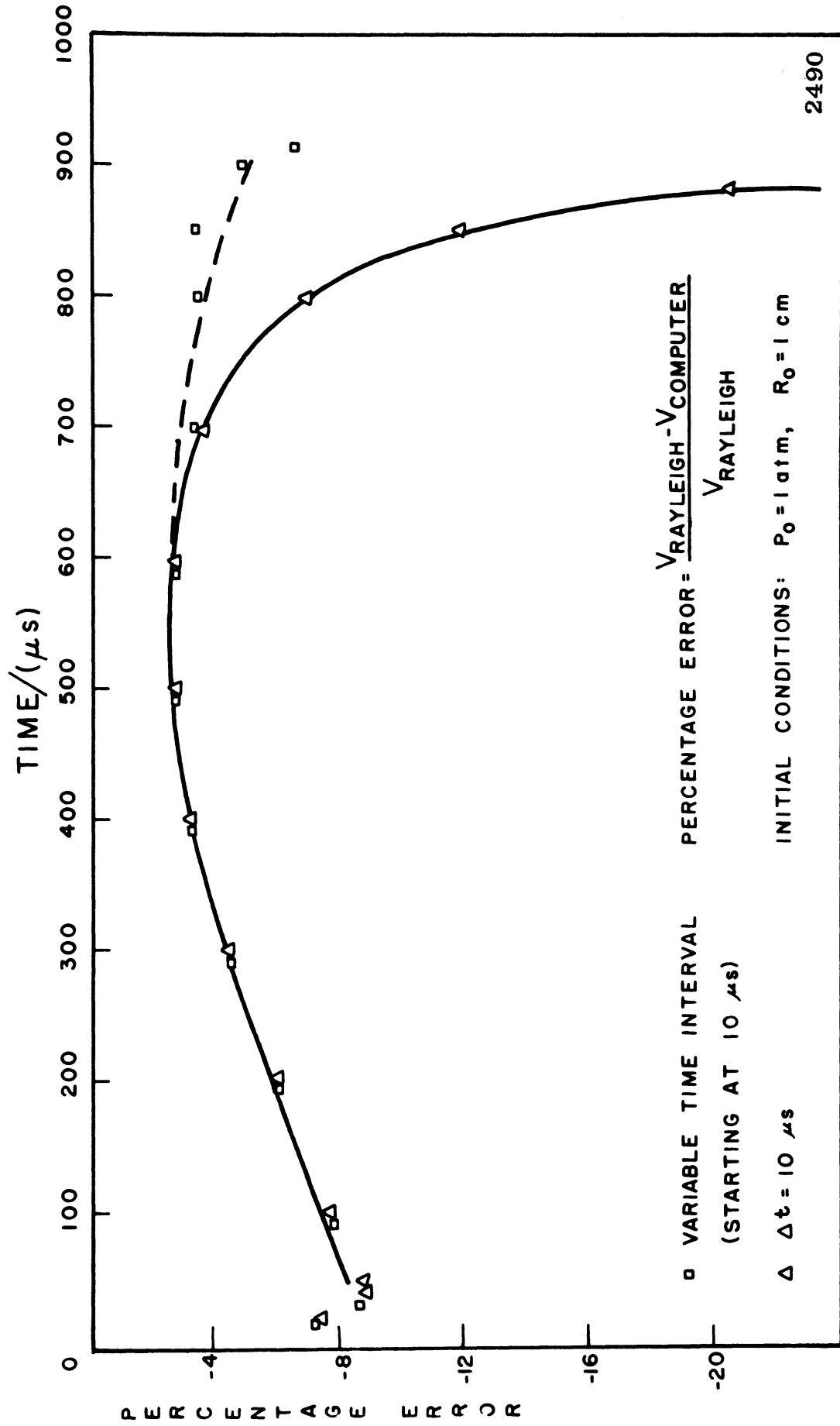
Fig. 3.--Effect of Variable Time Interval
on Accuracy of the MAC Method.

Experimental Considerations:

The objective of this part of the investigation is to determine
the detailed mechanism of the asymmetric mode of cavitation bubble
collapse. The asymmetry is introduced into the experimental system
by the presence of a solid wall. The previous experimental study under-
taken with a Fastax camera has been discussed in reference (14). Since
this initial investigation, several modifications have been made.

The major modification to the two-dimensional venturi used in this
investigation has been the attachment of a spoiler to the adjustable
bolt shown in Figure 4. By turning the bolt, the area of the spoiler
perpendicular to the flow can be changed; thereby, partially controlling
the division of flow at the tip of the wedge. Experimentation, while
taking pictures with both the Fastax and Dynafax cameras, showed that an
unequal division of flow at the tip of the wedge caused the separation
bubble shown in Figure 5. By placing the spoiler on the same side of
the wedge as the separation bubble, the flow division at the tip could
be equalized and the bubble nearly eliminated as shown in Figure 6.

Additional modifications of the venturi have been undertaken which
included gluing the four sides together and installing a plexiglas window
to facilitate adjustment and removal of the wedge. These modifications
serve the two-fold purpose of eliminating the leaks associated with the
multitude of seals previously required and of reducing the time required
for wedge adjustment by a factor of ten.
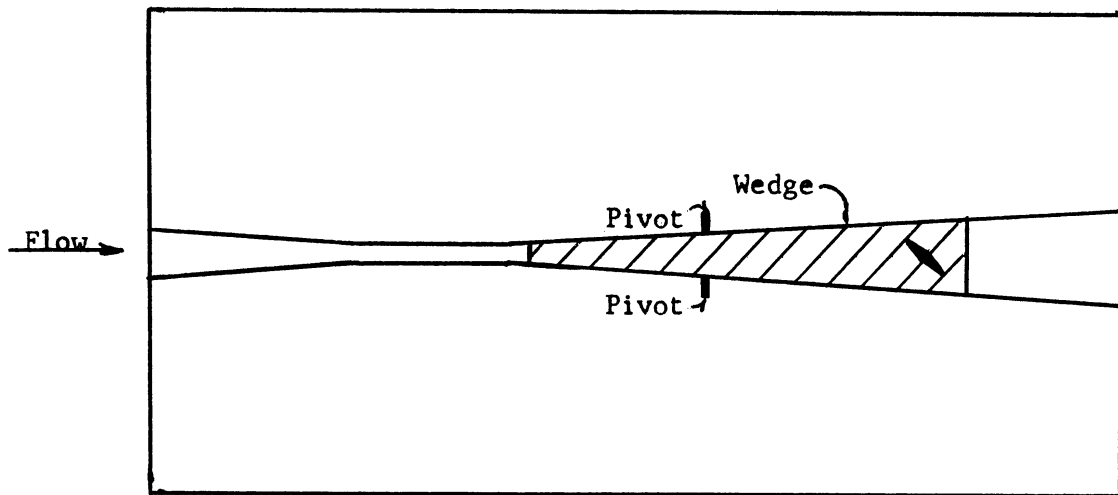
TOP VIEW
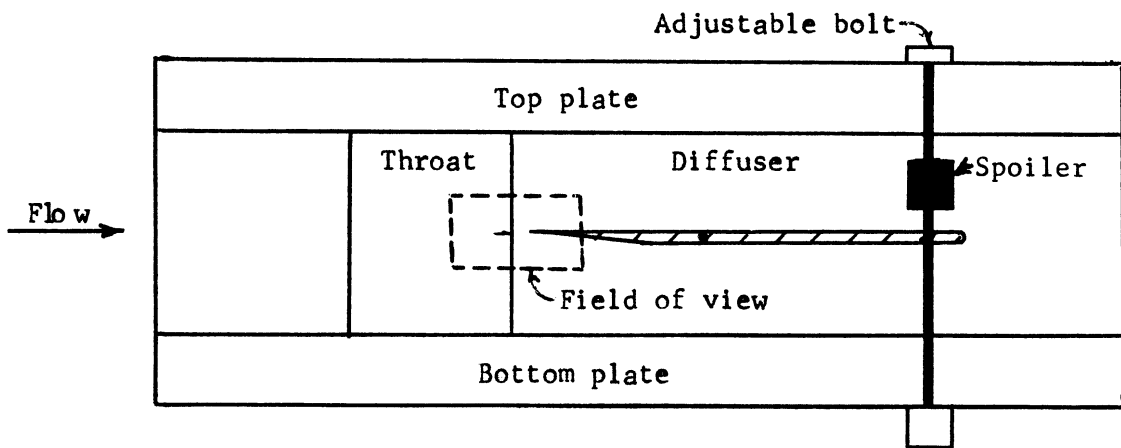
SIDE VIEW

2491

Fig. 4.--Wedge and Spoiler in Plexiglas
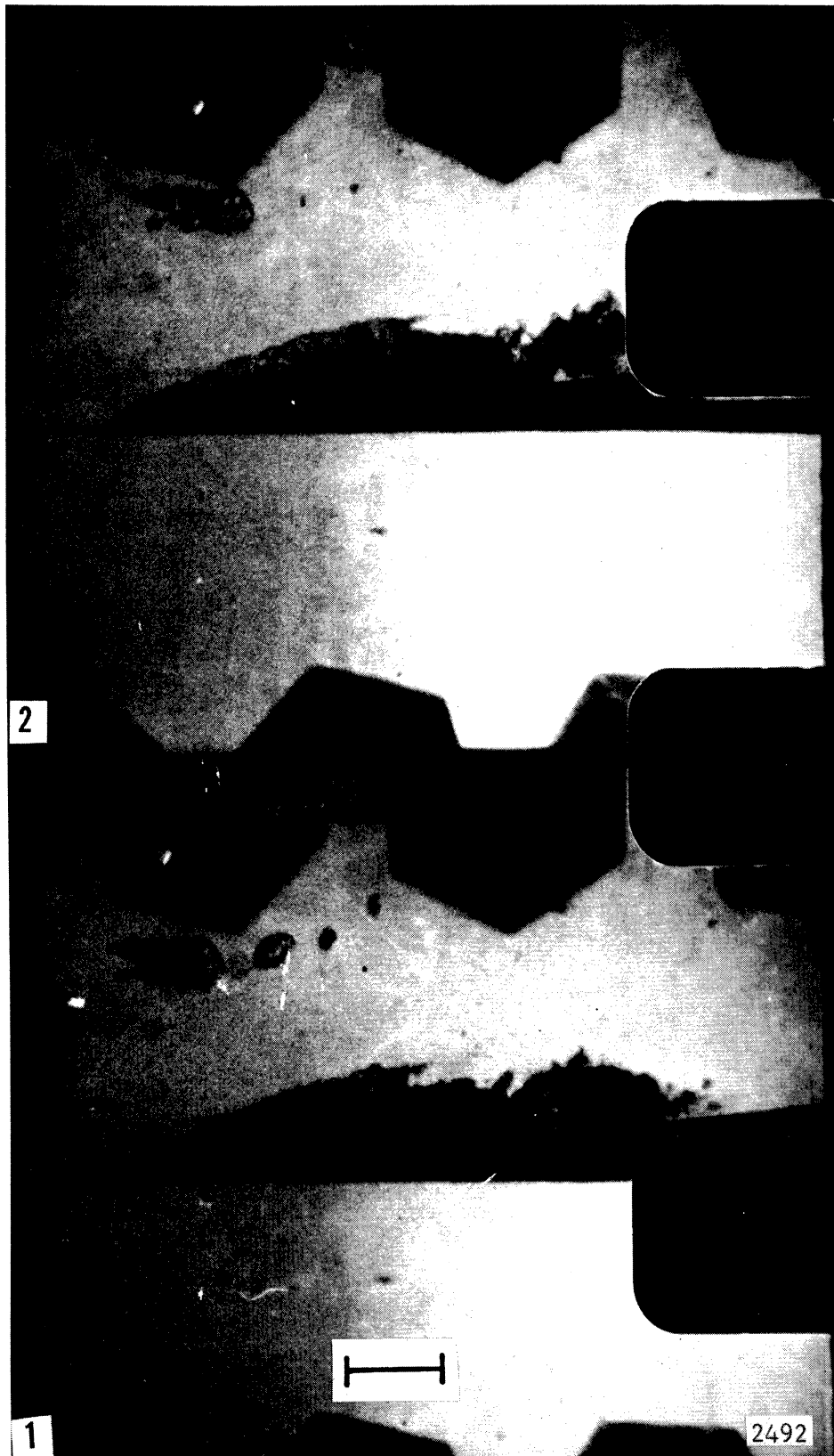Section of Two-Dimensional Venturi.

Fig. 5.--Dynafax Photographs Showing
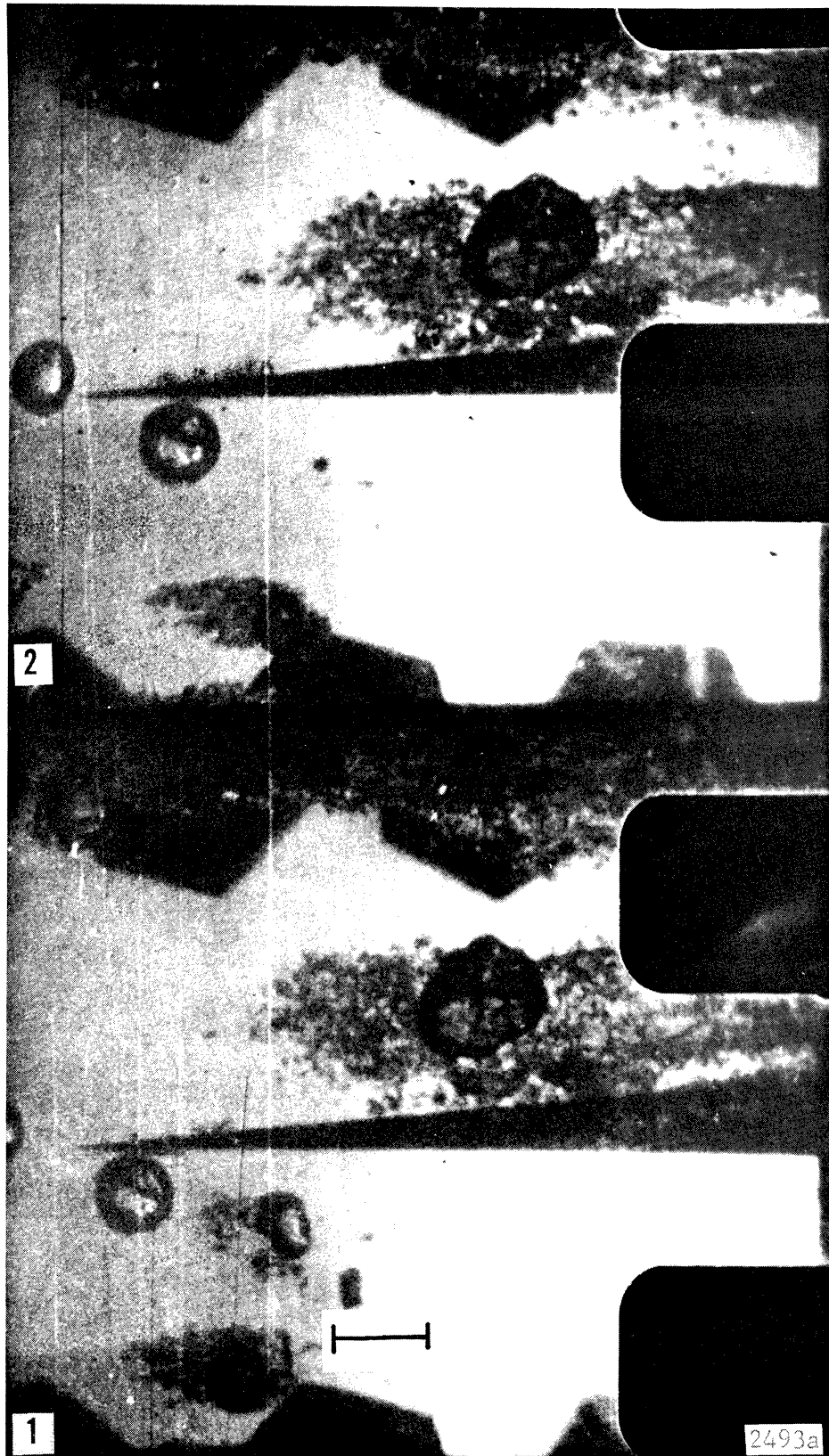Separation Bubble. 80 Microseconds per Frame,
Scale Length 1.0 cm.

Fig. 6.--Dynafax Photographs Showing
Elimination of Separation Bubble. 80 Micro-
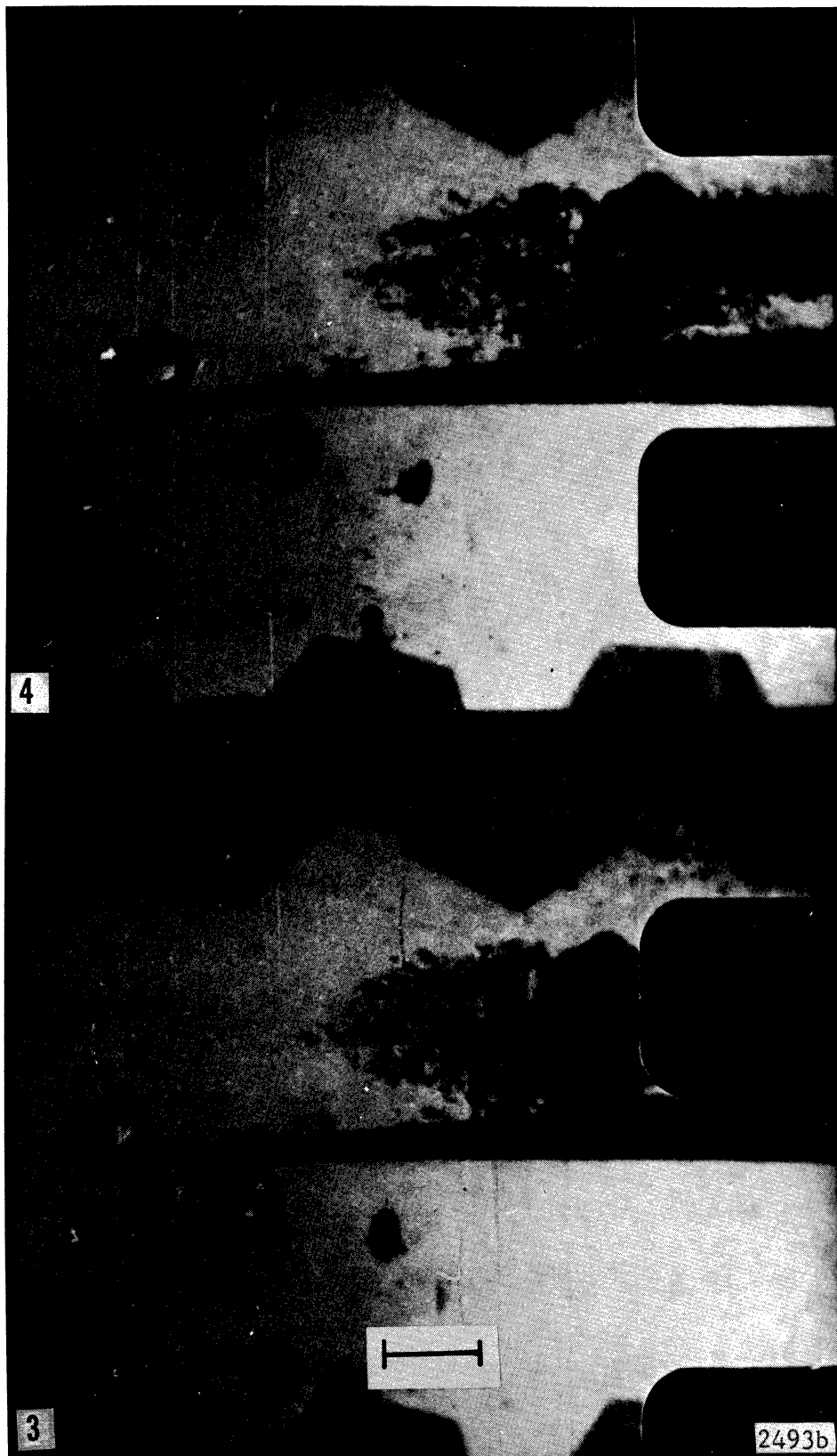seconds per Frame, Scale Length 1.0 cm.
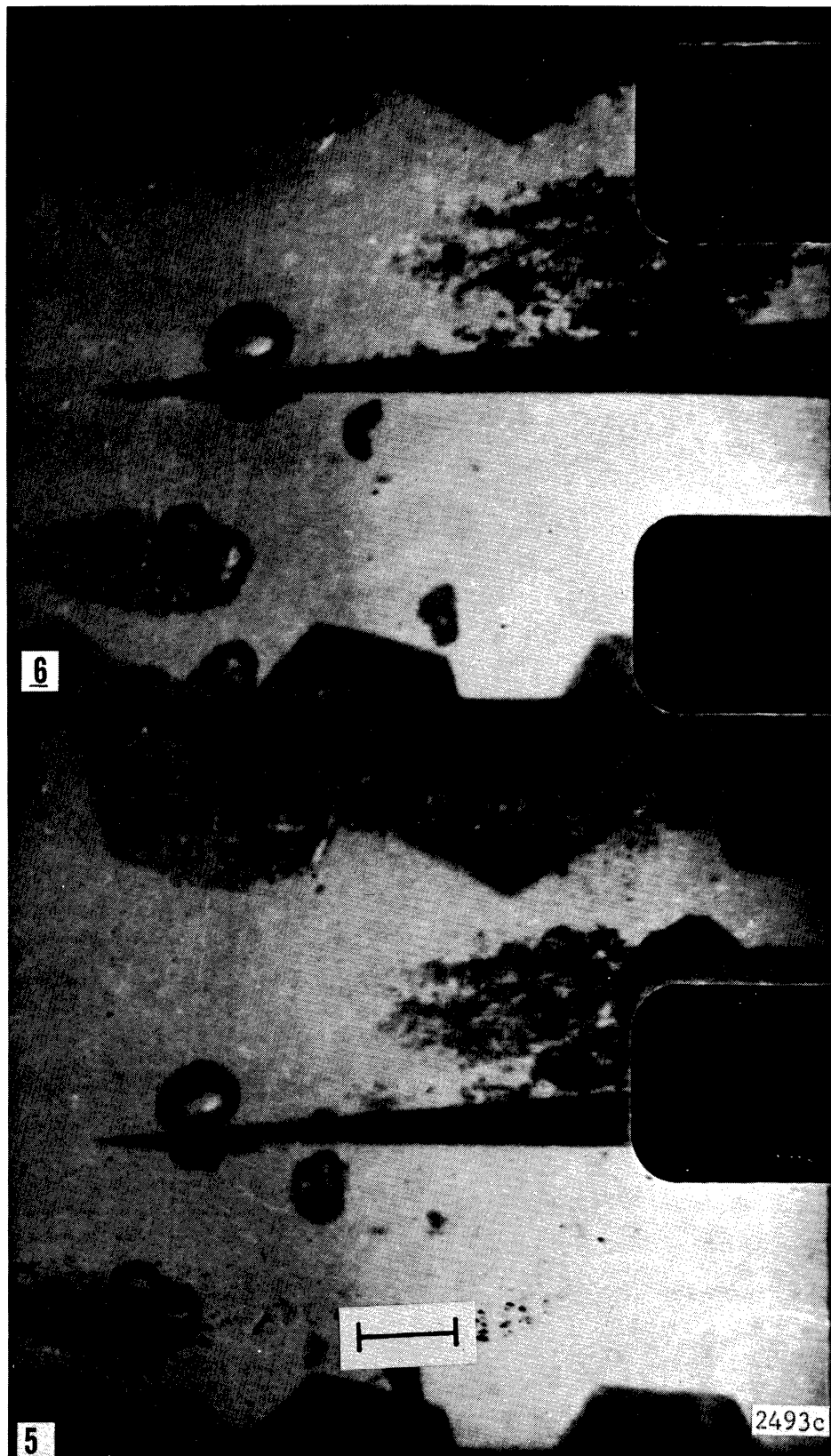
Fig. 6.--(Cont.)

Fig. 6.--(Cont.)

By the time tests were completed showing that the flow problem had
been resolved, the conclusion was reached that the Dynafax camera, although
offering a three fold increase in framing rate (25,000 frame per second
maximum) over the Fastax camera, still had neither the framing rate nor
the resolution required. Results obtained both with the Fastax and the
Dynafax cameras show that a bubble lifetime in the two-dimensional venturi
is on the order of 3 ms, while the final collapse phase occurs in both
cases in the time between frames, or less then 40 μs. Therefore, a
camera capable of photographing a bubble during this final collapse is
required. It may also be seen from the small size of the bubble during
the important final stages of collapse, that a camera with improved spatial
resolution, as compared with the Fastax and Dynafax cameras, is required.

Only a few types of cameras are capable of producing several photo-
graphs within a 40 μs period, i.e., framing rates of 10^5 frames per
second or greater. Ultra-high speed rotating mirror cameras are capable
of framing rates in the millions of frames per second with exposure times
on the order of the reciprocal of the framing rate. 35 mm film is generally
used, limiting negative image size and therefore resolution. Unless a
continuous access type of rotating mirror camera is employed, syncroni-
zation of the camera with the random occurrence of the cavitation bubbles
of this investigation would be possible. Spark cameras are capable of
framing rates in the millions of frames per second if a reliable delay

network can be constructed. Exposure times are equal to the duration of
the spark light source and are generally a fraction of a microsecond.
The only other common camera capable of such high framing rates is the
image converter camera. Both exposure time and framing intervals may
be measured in nanoseconds giving extremely high framing rates on the
order of 10^8 frames per second. However only a very small number of
frames, about 5, can be obtained and the spatial resolution is an order
of magnitude less that than obtainable with rotating mirror or spark
cameras.

A very high speed rotating mirror camera, having continuous access,
has been ordered for use in this investigation, but it will not be
available for at least six months. In order that the work may proceed
during this period, a specialized spark camera is being constructed.
A schematic of the camera is shown in Figure 7 and a picture of the
physical setup is shown in Figure 8. The camera uses a series of spark
light sources mounted in a circle. These spark light sources are con-
trolled by a twelve stage delay network. The network has an initial
delay that is continuously variable from 2 to 1000 μs with each successive
delay variable from 1 to 100 μs in seven steps. The effective framing rate
is from 10^4 to 10^6 frames per second. The pulse width (or exposure time)
of the discharging spark light source is approximately 0.2 μs.
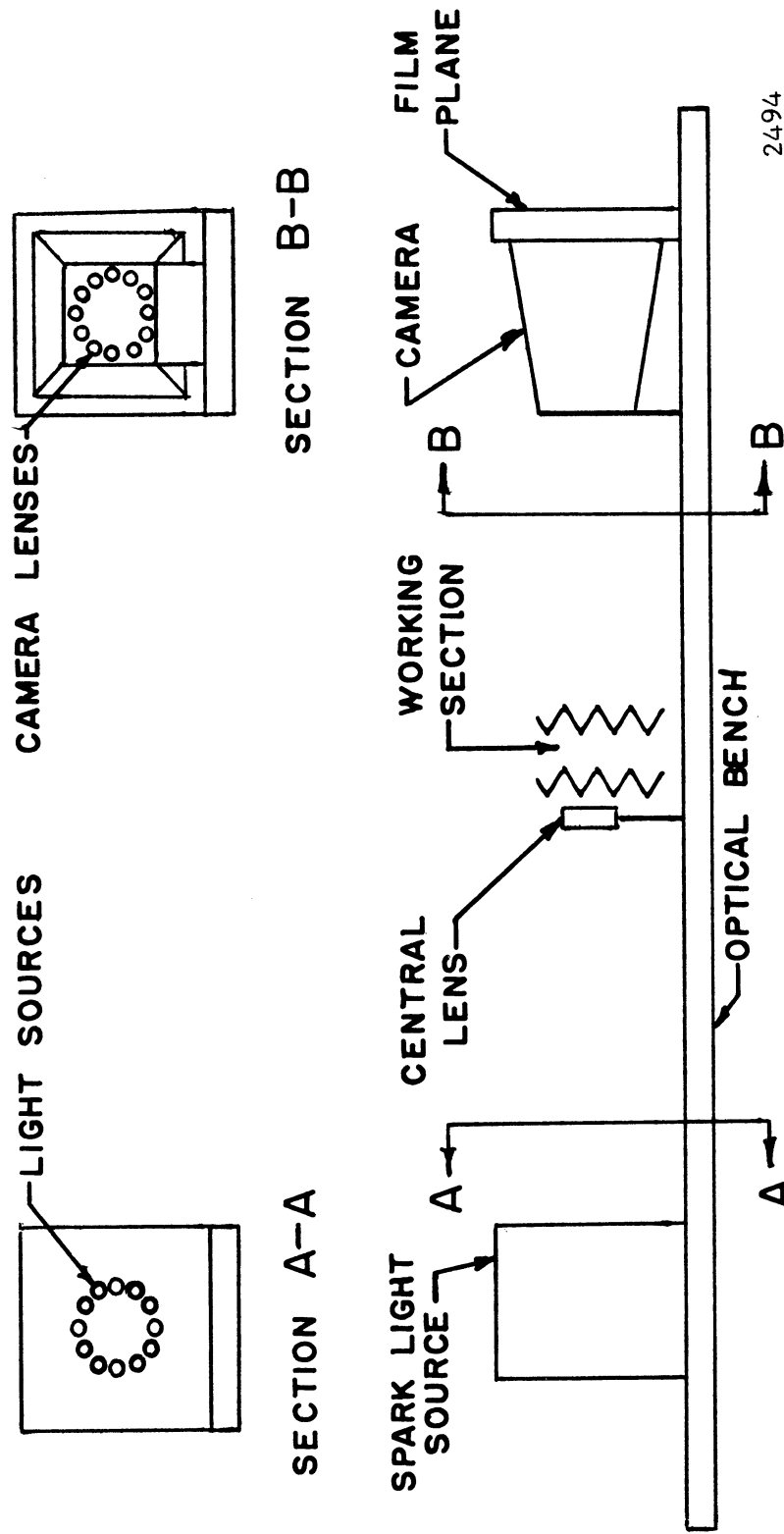
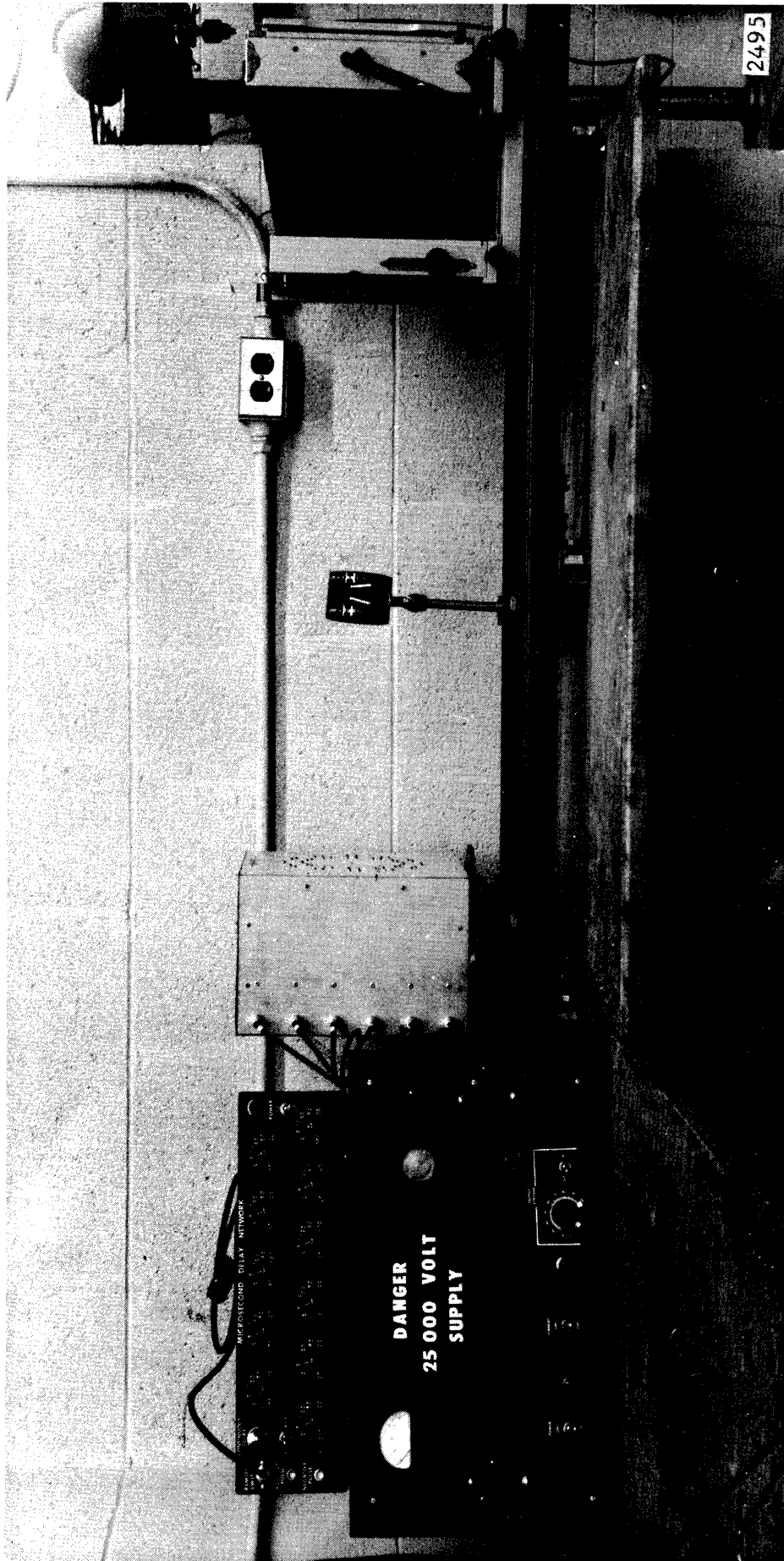Fig. 7.--Schematic Diagram of Spark Camera.

Fig. 8.--Spark Camera Including Delay Network and High Voltage Power Supply.

The light from each light source is focused by the large central lens onto one of the camera lenses. There is a camera lens for each light source and the optical system is arranged so that the camera lenses and light sources are mounted at the same radius. In turn, the camera lenses focus the working section on the stationary film plane. The resulting negative has a circle of images on a radius slightly greater than the camera lenses. The camera is capable of holding 8 inch x 10 inch sheet film in order to obtain negative images as large as possible.

A representative sequence of pictures from the initial use of this camera shows a liquid jet emerging from an orifice and impacting on a plexiglas specimen (Figure 9). The high resolution and short exposure time of this camera are plainly evident. The major limitation of this camera, for our work, is the low number of frames per run, 12. This limitation is imposed by the physical size of the spark sources used and the need to make the negative images as large as possible. It may be possible to partially overcome this disadvantage by providing some means of detecting a bubble in its latter stages of collapse and then starting the camera with this detector. Other limitations of this camera not pertinent to our work are that its use is restricted to subjects which are non-luminous and can be back lighted.
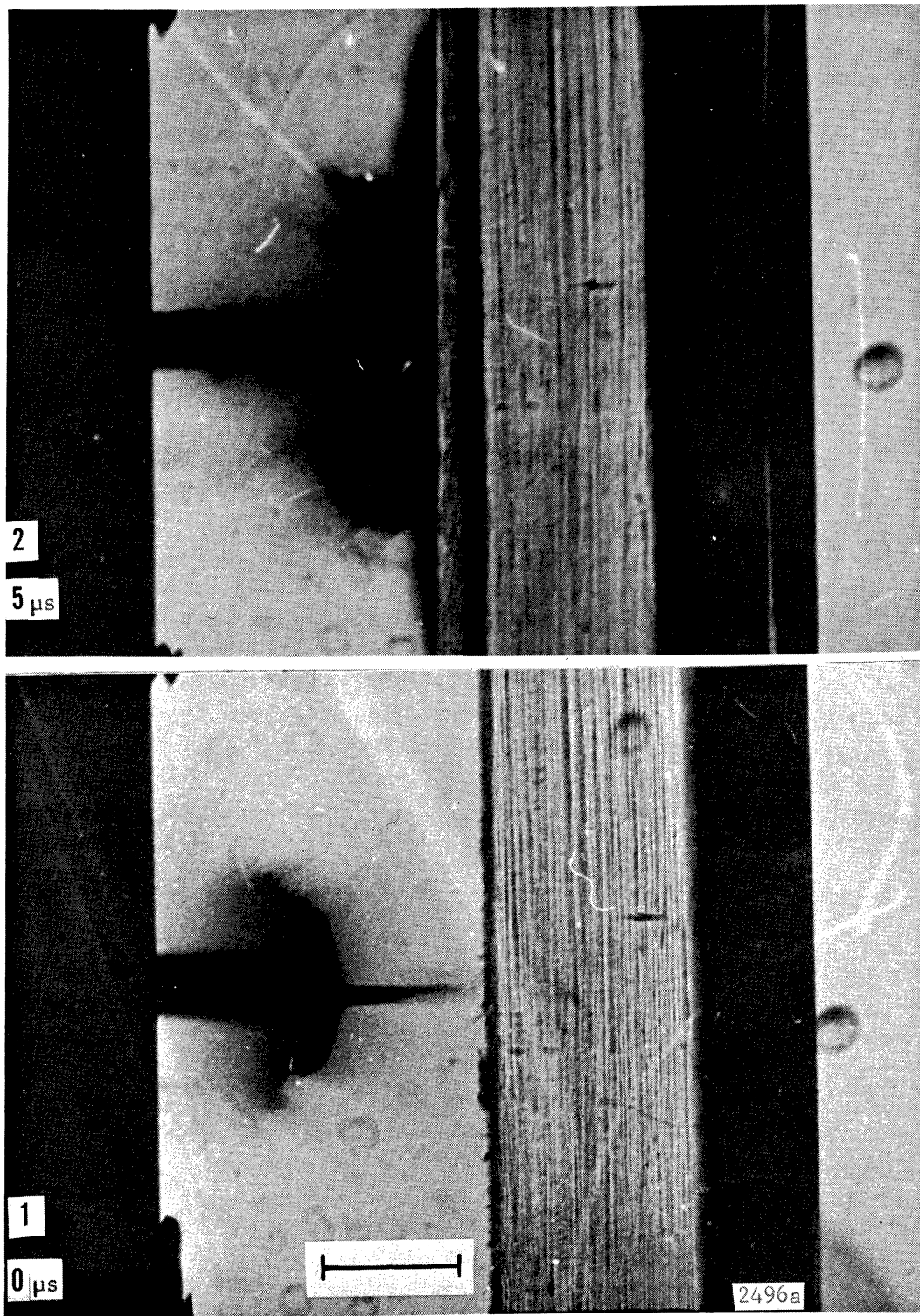
Fig. 9.--Spark Camera Photographs Showing
Water Jet Impacting on a Plexiglas Specimen.
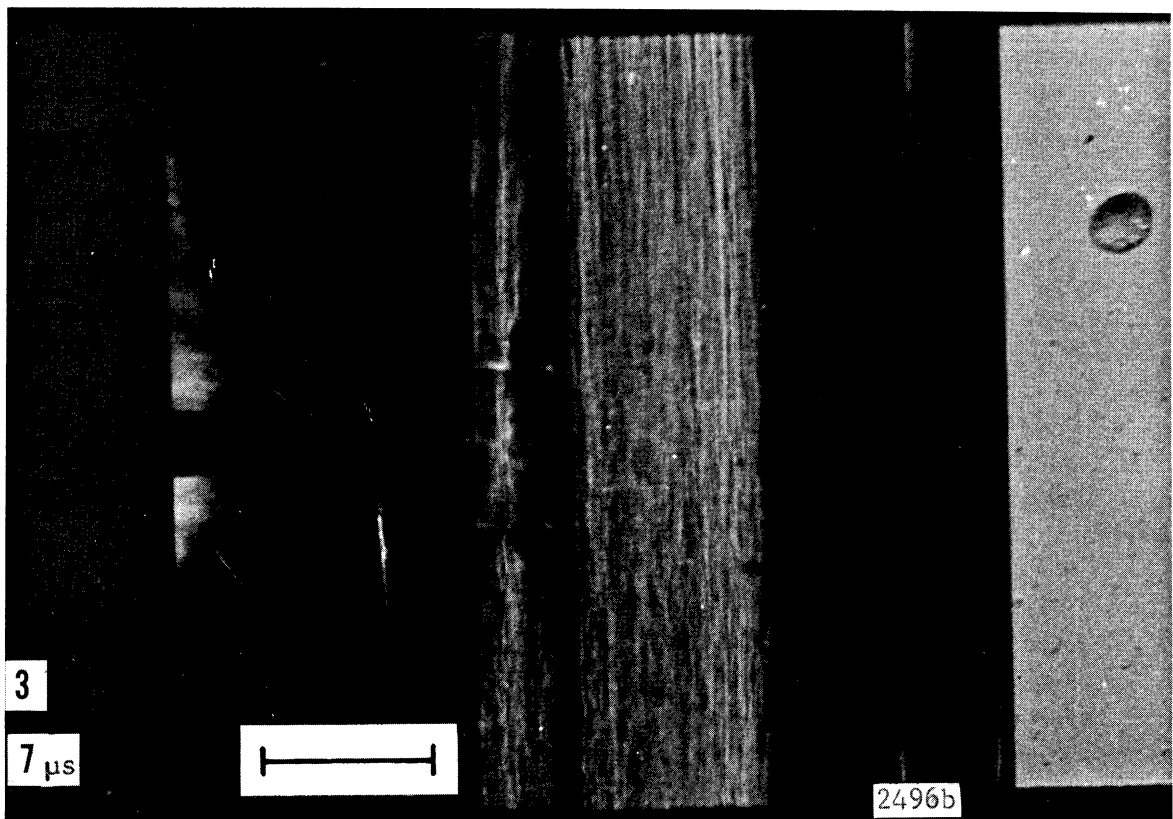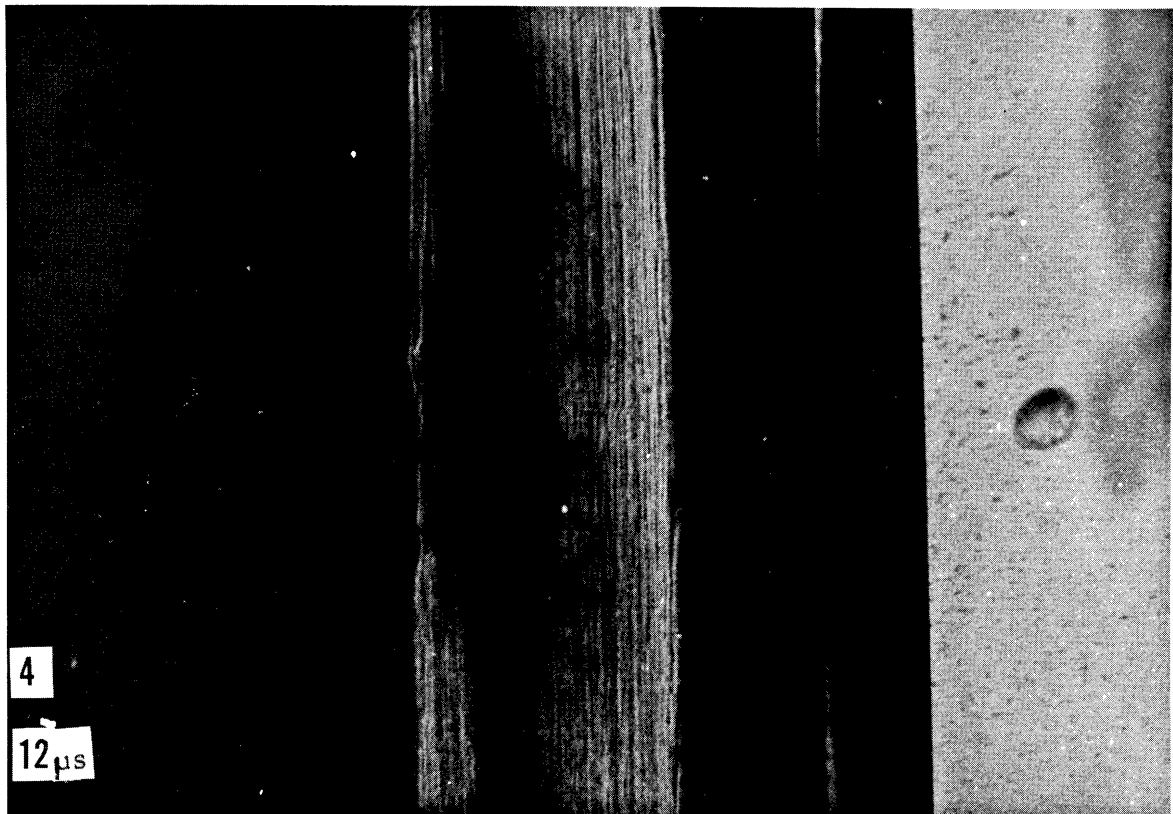Time in Microseconds Measured from Frame Number 1,
Scale Length 0.5 cm.

Fig. 9.--(Cont.)

The high speed rotating mirror camera which will eventually be available for this work will have a maximum framing rate of 2×10^6 frames per second and a total of 82 frames per sequence. The image size will be somewhat smaller than that obtained with the spark camera, causing a corresponding reduction in resolution, but this is not expected to be a serious limitation.

BIBLIOGRAPHY

1. Lord Rayleigh, "On the Pressure Developed in a Liquid During the Collapse of a Spherical Cavity," Phil. Mag., 34, (1917) 94-98.

2. Hickling, R. and Plesset, M., "Collapse and Rebound of a Spherical Bubble in Water," The Physics of Fluids, 7, No. 1, (1964) 7-14.

3. Ivany, R. D. and Hammitt, F. G., "Cavitation Bubble Collapse in Viscous, Compressible Liquids - Numerical Analysis," J. Basic Eng., Trans. ASME, D, 87, (1965) 977-985.

4. Kornfeld, M. and Suvorov, L., "On the Destructive Action of Cavitation," J. Applied Physics, 15, No. 6, (1944) 495-506.

5. Rattray, M., "Perturbation Effects in Cavitation Bubble Dynamics," Cal. Inst. of Tech., Ph.D. Thesis, 1952.

6. Naude, C. F. and A. T. Ellis, "On the Mechanism of Cavitation Damage by Nonhemispherical Cavities Collapsing in Contact with a Solid Boundary," Trans. ASME, J. Basic Eng., (1961) 648-656.

7. Shutler, N. D. and Mesler, R. B., A Photographic Study of the Dynamics and Damage Capabilities of Bubbles Collapsing Near Solid Boundaries, Trans. ASME, J. Basic Eng., D, 87, (1965) 511-517.

8. Benjamin, T. B. and Ellis, A. T., "The Collapse of Cavitation Bubbles and the Pressures Thereby Produced Against Solid Boundaries," Trans. Royal Society, A, 260, (1966) 221-240.

9. Ivany, R. D., Hammitt, F. G., and Mitchell, T. M., "Cavitation Bubble Collapse Observations in a Venturi," J. Basic Eng., Trans ASME, D, 88, (1966) 649-657.

10. Yeh, H., "The Dynamics of Gas Bubbles Moving in Liquids with Pressure Gradient," Ph.D. Thesis, University of Michigan, 1967.

11. Harlow, F. H., "The Particle-in-Cell Computing Method for Fluid Dynamics," Methods in Computational Physics, 3, (1964) 319-343.

12. Welch, J. E., Harlow, T. H., et al, "The MAC Method: A Computing Technique for Solving Viscous Incompressible Transient Fluid - Flow Problems Involving Free Surfaces," Los Alamos Scientific Laboratory Report LA-3425 (March, 1966).

Lamb, Sir Horace, <u>Hydrodynamics</u>, Dover Publ., 6th Ed., New York, (1945) 7.

Mitchell, T. M., Kling, C. L., and Hammitt, F. G., "Bubble Collapse Behavior Around a Sharp Wedge in a Diffuser," Department of Nuclear Engineering Laboratory for Fluid Flow and Heat Transport Phenomena, University of Michigan, Report No. 07738-T-1, July, 1966.